ORIGINAL RESEARCH

Electroacupuncture Pretreatment Ameliorates Anesthesia and Surgery-Induced Cognitive Dysfunction via Activation of an α7-nAChR Signal in Aged Rats

Zhigang Wang[1,2]
Tianlin Liu [1]
Chunping Yin[1]
Yanan Li[1]
Fang Gao[1]
Lili Yu[1]
Qiujun Wang [1]

[1]Department of Anesthesiology, The Third Hospital of Hebei Medical University, Shijiazhuang City, Hebei, People's Republic of China; [2]Department of Anesthesiology, Handan Central Hospital, Handan, Hebei, People's Republic of China

Objective: Postoperative cognitive dysfunction (POCD) after anesthesia and surgery (AS) is a common complication in the elderly population. A cholinergic-dependent signal, the alpha7-nicotinic acetylcholine receptor (α7-nAChR), has been suggested to regulate cognitive processes in a variety of neurologic diseases. In the current study, we determined whether electroacupuncture (EA) pretreatment ameliorates AS-induced POCD in aged rats, as well as the underlying mechanism.

Methods: Male Sprague-Dawley rats (20 months old) were randomly assigned to the following 5 groups (n=12): vehicle; POCD (tibial fracture surgery); EA plus POCD; EA plus POCD and alpha-bungarotoxin (α-BGT); and POCD plus α-BGT groups. Alpha-bungarotoxin (1 μg/kg), a selective antagonist of α7-nAChR, was administrated via intraperitoneal injection before EA. Thirty days post-AS, the Morris water maze and a novel objective recognition test were used to evaluate cognitive function. Neuronal amount, apoptosis, microglial activation, percentage of high mobility group box 1 (HMGB1)- and nuclear factor-κB (NF-κB)-positive microglia, and levels of HMGB-1 downstream factors, including NF-κB, interleukin-6 (IL-6), and IL-1β, were detected by Nissl staining, immunofluorescence, and Western blot assays.

Results: EA pretreatment significantly increased crossing platform times and elevated the time with a novel object, restored the quantity of neurons, decreased TUNEL-positive neurons, alleviated activation of microglia, downregulated expression of HMGB1 and NF-κB in the microglia, and reduced levels of phosphor-NF-κB, IL-6, and IL-1β 35 days after AS, while α-BGT partially reversed these changes.

Conclusion: EA pretreatment improved AS-induced POCD in aged rats, and the underlying mechanism may be associated with inhibition of HMGB1–NF-κB via an α7-nAChR signal in the microglia.

**Keywords:** electroacupuncture, EA, postoperative cognitive dysfunction, POCD, α7-nicotinic acetylcholine receptor, α7-nAChR, microglia, high mobility group box 1, HMGB1

Introduction

Postoperative cognitive dysfunction (POCD), which involve concentration, attention, or memory impairment, have been reported to be a common complication after anesthesia and surgery (AS).[1,2] POCD is more frequently associated with increased mortality in the elderly population.[3,4] POCD, an age-associated perioperative

Correspondence: Qiujun Wang
Tel +86 311 8860 2072
Email wangqiujunsy@163.com

Graphical Abstract
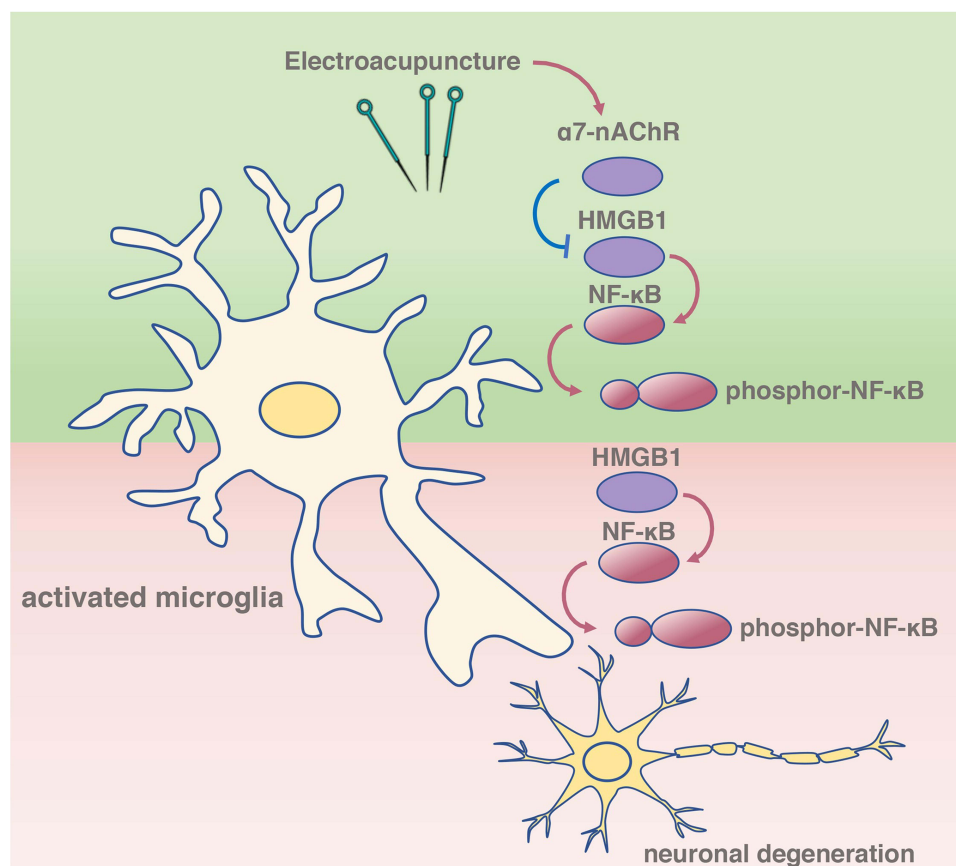
complication, has become a worldwide problem affecting the family and community in addition to the aging.[5] Until now, the pathogenic mechanism underlying POCD remains unclear, and available means to prevent and cure POCD are still lacking.

Previous studies have demonstrated that the stress response induced by surgical treatment with anesthesia leads to an inflammatory reaction in the central neuronal system.[6,7] Inhaled anesthetics, including isoflurane and sevoflurane, have been reported to induce inflammatory reactions in the hippocampus, which in turn lead to cognitive impairment in aged rats.[8,9] Moreover, surgical treatment in mice, as well as mechanical ventilation, further result in chronic neuroinflammation and aggravate cognitive impairment.[10,11] Acupuncture, a traditional Chinese medicine therapeutic technique, has been suggested to restore homeostatic balance and have anti-inflammatory effects.[12] Recently, electroacupuncture (EA), which has a controllable stimulation frequency and intensity, exerts preventive effects against cognitive dysfunction in rodent

models of POCD.[13,14] In addition, a previous study from our group showed that EA improves cognitive decline in elderly patients with a focal lacunar infarction;[15] however, the mechanism underlying EA against POCD in elderly patients remains to be determined.

It has been reported that EA incites an anti-inflammatory cholinergic-dependent signal, the alpha7-nicotinic acetylcholine receptor (α7-nAChR), thus suggesting neuroprotective effects against cerebral ischemia-reperfusion injury.[16,17] In addition, activation of α7-nAChR ameliorates radiation-induced lung injury and zymosan-induced acute kidney injury via inhibition of the high-mobility group box 1 (HMGB1)–nuclear factor-κB (NF-κB) pathway.[18,19] Interestingly, EA has also been reported to ameliorate neuropathic pain via suppression of the HMGB1/NF-κB signal in the spinal cord.[20] HMGB1, an abundant inflammatory protein in the brain, is likely to involved in the pathogenesis of cognitive decline-associated diseases.[21] NF-κB, as a downstream signal of HMGB1, can induce the transcription of multiple

inflammatory factors.[22] Currently, the roles of α7-nAChR and HMGB1–NF-κB in EA against AS-induced POCD is unclear.

The current study determined whether EA pretreatment ameliorates POCD in a rodent model of tibial fracture surgery. In addition, the roles of the α7-nAChR–HMGB1–NF-κB signal under POCD condition was further investigated.

Methods

All experiments involving animals were performed according to the National Institute of Health Guideline for the Care and Use of Laboratory Animals. The protocols involving animals were also approved by the Animal Review Board of Hebei Medical University.

Group Assignment

Male Sprague-Dawley rats were randomly assigned to one of the following five groups (computer-based randomization): (1) vehicle; (2) POCD; (3) EA + POCD; (4) alpha-bungarotoxin (α-BGT) + EA + POCD; and (5) α-BGT + POCD. Rats in the POCD group were subjected to tibial fracture surgery. EA pretreatment was performed once a day for 5 days and were subjected to POCD 24 h after the last treatment. Alpha-bungarotoxin (catalog # HY-P1264; MedChemExpress, Newark, NJ, USA), a specific α7-nAChR antagonist, was administrated via intraperitoneal injection 30 min before EA pretreatment for 5 days. Alpha-bungarotoxin (1 µg/kg dissolved in sodium chloride at a concentration of 150 mM) was used based on a previous study[23] and our preliminary experiments. Sodium chloride (150 mM) was administrated via intraperitoneal injection to the POCD and EA + POCD groups as a vehicle treatment (Figure 1A).

POCD Model

Male Sprague-Dawley rats (20 months old) were used to establish the POCD model following tibial fracture surgery.[24] Before surgical treatment, the rats were kept in separate cages with wood shavings at 20–22°C with an alternating 12 h day–night cycle (40–60% of humidity) and permitted access to water and food ad libitum. Rats were kept in an anesthetic box filled with 7–8% sevoflurane as an induction agent, then placed on a warming pad (3–4% sevoflurane for anesthetic maintenance at 36–38°C). Following shaving and disinfection, a median incision was performed on the left-hind paw, and the tibial periosteum was stripped. After a tibial osteotomy was

performed, a pin (diameter, 0.38 mm) was inserted into the intramedullary canal and the wound was sutured with silk thread. The rats in the vehicle group were only treated with a skin incision and suture on the left-hind paw following anesthesia.

Electroacupuncture Pretreatment

An electronic acupuncture treatment device (Model G6805; SMIF, Shanghai, China) was used to practice EA treatment. In brief, after anesthetic induction with 7–8% sevoflurane, EA pretreatment at the Hegu, Neiguan, and Zusanli acupoints was performed at a frequency of 2–15 Hz. In addition, the EA intensity was performed during a moderate muscle contraction. Hegu (LI4) is situated between the first and second metacarpal bones, Neiguan (PC6) is located approximately 3 mm from the transverse stripe of the wrist at the axopetal end, and Zusanli (ST36) is located approximately 5 mm lateral to the anterior tubercle of the tibia[25] (Figure 1B). The rats in the vehicle and POCD groups received acupuncture, but were not stimulated.

Novel Object Recognition (NOR)

Thirty days after AS treatment, we assessed the ability of cognition using a NOR test. At 28 and 29 days after surgical treatment, rats were allowed to freely explore an empty black box (60 × 60×40 cm) for 5 min/d for 2 days as the adaptation phase. At 30 days, rats were allowed to explore the same two cubic objects, which were located in the left and right corners of the black box. The exploration phase was 5 min in duration. Then, the right cubic object was removed and replaced with a novel spherical object. During this phase, continuous monitoring recorded by a video analysis system (XR-XZ301; Xinruan, Shanghai, China) was performed for 5 min. The recognition index (RI) was used to analyze the cognitive ability, as follows: RI = novel object exploration time/(novel object exploration time + familiar object exploration time).

Morris Water Maze Test

At 31 days after surgical treatment, we evaluated the ability of memory and learning using the Morris water maze test. In brief, rats were placed in a circular container (diameter, 200 cm) filled with warm water (temperature, 25 ± 1 °C). During the acquisition phase, rats were allowed to look for a transparent platform which was placed below the water (depth, 0.5 cm). In addition, we suspended distinctive distal visual cues surrounding the
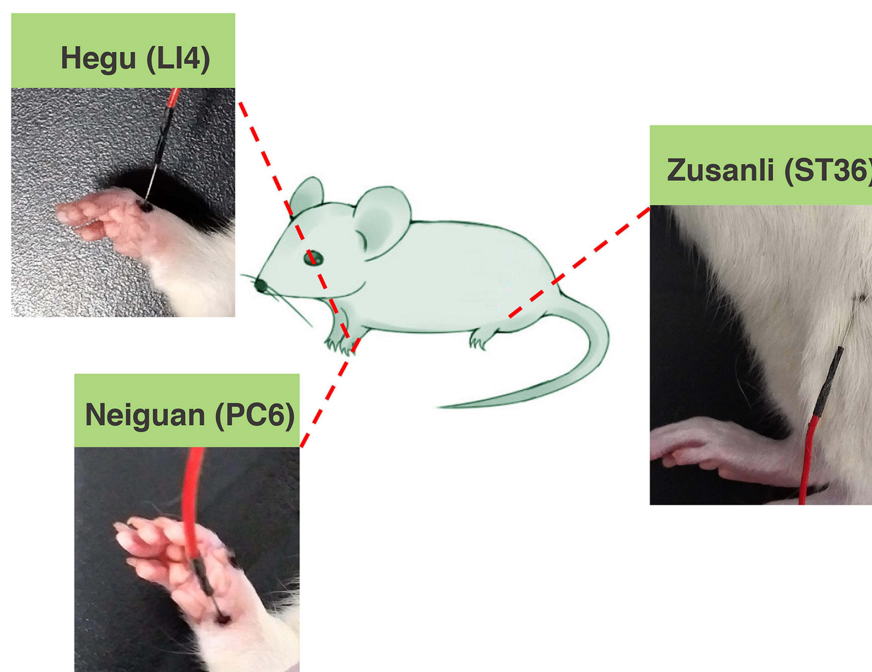
A
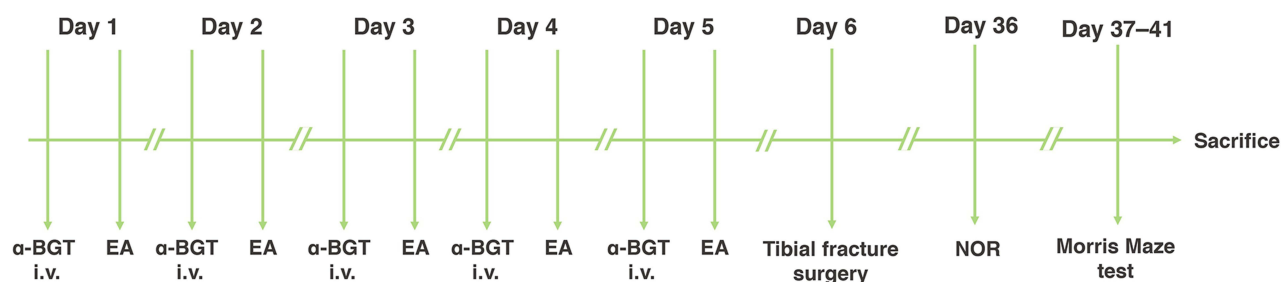
B

Figure 1 The experimental schematic diagram. (**A**) Rats were treated with EA pretreatment once a day for 5 days and were subjected to tibial fracture surgery 24 h after the last treatment. Alpha-bungarotoxin (α-BGT) was administrated via intraperitoneal injection 30 min before EA pretreatment for 5 days. After NOR and Morris maze tests were evaluated, rats were sacrificed. (**B**) EA pretreatment was carried out at the Hegu (LI4), Neiguan (PC6) and Zusanli acupoints (ST36).
Abbreviations: EA, electroacupuncture; NOR, novel object recognition.

container in the experimental room until the end of the study. The training test was performed from quadrants I–IV every day and continued for 4 days. The rats were trapped on the platform for 30 s if unable to climb the platform within 90 s. Thirty-five days post-AS, the platform was retracted from the pool. We recorded the latency to the platform, the number of times the platform was crossed, the total time, and the distance spent in the target quadrant.

Nissl Staining

At the end of the Morris water maze test (n =6), brains were removed under anesthesia with sevoflurane, then cerebral tissue containing the hippocampus were fixed in

4% paraformaldehyde. Following dehydration and embedding, we sectioned the brains at a thickness of 4 μm. After dewaxing and hydrating at room temperature, the slices were treated with Nissl staining solution (C0117; Beyotime, Shanghai, China). Under a light microscope (BX51; Olympus, Tokyo, Japan), the total Nissl body count in the dentate gyrus was analyzed by a pathologist blinded to grouping (three sections per section).

Immunofluorescence

The hydrated slices were processed by antigen retrieval, then a blocking reagent. The slices were treated with primary polyclonal goat against Iba1 antibody (1:200 dilution, ab5076; Abcam, Cambridge, UK), polyclonal rabbit

antibody against HMGB1 (1:100 dilution, AF0180; Beyotime), and phosphor-NF-κB (1:100 dilution, AF2006; Affinity Bioscience, OH, USA) overnight at 4°C. The next day, the slices were processed using corresponding secondary antibodies. After rising with PBS, the cell nuclei were colored by 5 µg/mL of DAPI (P0131; Beyotime).

For the TUNEL staining assay, the hydrated slices were incubated with protease K (20 µg/mL, ST533; Beyotime) at 37 °C for 35 min was used to determine apoptosis of the neuron. Then, the slices were treated with antigen retrieval, blocking reagent, polyclonal mouse antibody against NeuN (1:200 dilution, ab104224; Abcam), CyTM3-conjugated goat anti-mouse IgG (1:500, A0521; Beyotime), and TDT enzyme containing fluorescent labeling solution (C1088; Beyotime).

A fluorescence microscope (MF31; Mshot, Guangzhou, China) was used to assess the above slices by a pathologist blinded to grouping. Six fields with a magnification of ×200 in 3 slices were randomly selected from each group. The percentage of HMGB1- and Iba1-positive cells and phosphor-NF-κB- and Iba1-positive cells were analyzed by Image-Pro Plus 6.0 (NIH, Bethesda, MD, USA). Sholl analysis was performed to assess branch tips in a given microglia indicated by Iba1-positive cells. In addition, we evaluated neuronal apoptosis, which was defined as TUNEL- and NeuN-positive cells.

Western Blot

At the end of the Morris water maze test (n =6), total protein was extracted from hippocampal tissues under anesthesia with sevoflurane. SDS-PAGE (8%) for NF-κB and SDS-PAGE (12%) for IL-6 and IL-1β were used to perform electrophoresis. Then, the protein was shifted onto a PVDF membrane. After blocking, the PVDF membranes were processed by rabbit anti-rat phospho-NF-κB (1:1000 dilution, AF2006; Affinity Bioscience, OH, USA), rabbit anti-rat polyclonal NF-κB (1:1000 dilution, AF7569; Beyotime, China), mouse anti-rat Monoclonal IL-6 (1:1000 dilution, AF0201; Beyotime, China), and rabbit anti-rat polyclonal IL-1β (1:500 dilution, K101295P; Solarbio, China) at 4°C overnight. Next day, the PVDF membranes were processed by corresponding secondary antibodies (goat anti-rabbit antibody, 1:1000 dilution, A0516; Beyotime; goat anti-mouse antibody, 1:1000 dilution, A0521; Beyotime) at 25°C for 1 h. In addition, the internal reference was performed by a polyclonal rabbit anti-rat GAPDH (1:1000 dilution,

K200057M; Solarbio, Beijing, China). Following rising with TBS-T and incubation with ECL (P0018AM; Beyotime), we quantified protein bands on the PVDF membranes with Image-Pro Plus 6.0 software.

Statistical Analysis

Data are indicated as the mean ± standard deviation (SD). All statistical analyses were performed using SPSS software (version 17.0). For data with a normal distribution, one-way analysis of variance (ANOVA) was performed to evaluate differences followed by Tukey's multiple comparison test. For a non-normal distribution, the Kruskal–Wallis test was performed to evaluate differences followed by a Dunn-Bonferroni test. Two-way repeated-measures ANOVA followed by Tukey's post hoc test was used to analyze the escape latency during training days. Statistical significance was determined as a $P < 0.05$.

Results
Electroacupuncture Pretreatment Alleviates POCD in Aged Rats

Because rats have an innate tendency to probe new objects, novel object recognition was used to judge cognition and memory. In the familiarization phase, there was no significant difference in the total time spent between the right or left identical objects in the five groups (Figure 2B). In the testing phase, the rats treated with tibial fracture surgery exhibited a reduced RI calculated from time measures compared with the rats treated with vehicle ($P < 0.0001$; Figure 2A and C); however, EA pretreatment significantly increased the RI in the EA + POCD group compared to the POCD group ($P < 0.05$; Figure 2A and C), while α-BGT partially reversed the increase ($P < 0.01$; Figure 2A and C). There was no difference in the RI between aged rats in the POCD, EA + POCD and α-BGT + POCD groups (Figure 2A and C). In addition, there was no significant difference in the total distance and average speed between rats in the above five groups (Figure 2D and E).

To further examine learning and memory in aged rats, the Morris maze water test was performed after the NOR test. There was no significant difference in escape latency on day 1 between rats in the 5 groups, but the rats exposed to tibial fracture surgery in the POCD group had a longer latency period than the rats in the vehicle group from days 2–4 after AS ($P < 0.05$; Figure 2F and G). EA pretreatment before AS significantly decreased latency period to locate
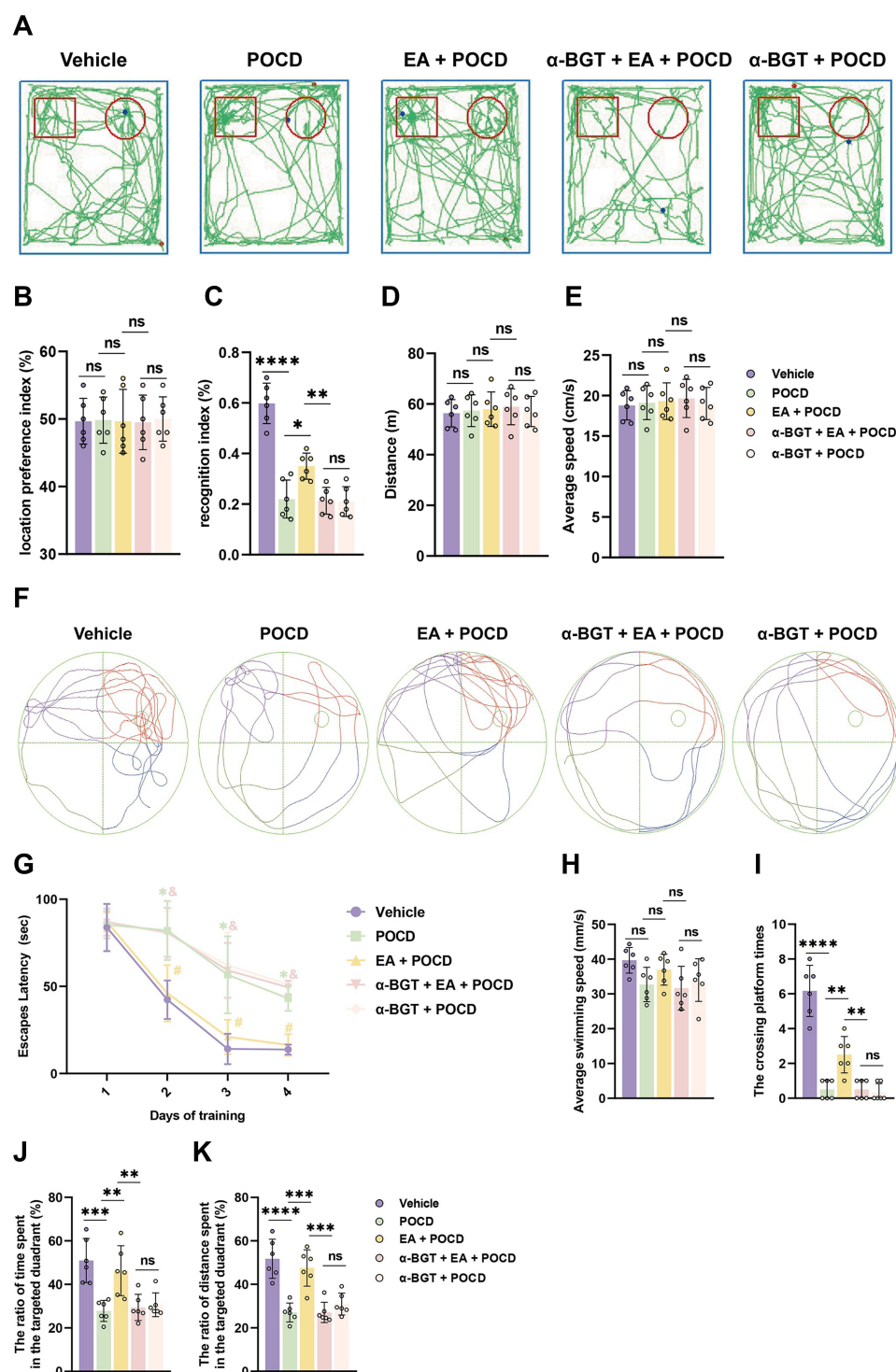
Figure 2 Electroacupuncture pretreatment alleviates POCD in aged rats. (**A**) Computer printouts of shift trajectories in the NOR caused by the indicated stimuli. (**B**) Location preference index in familiarization phase caused by the indicated stimuli. (**C**) Recognition index (RI) in testing phase caused by the indicated stimuli. (**D**) Total distance in testing phase caused by the indicated stimuli. (**E**) Average speed in testing phase caused by the indicated stimuli. (**F**) Computer printouts of shift trajectories in the Morris maze test caused by the indicated stimuli. (**G**) Escape latency in the training phase caused by the indicated stimuli. (*P <0.05 versus Vehicle group, #P <0.05 versus POCD group, &P <0.05 versus EA + POCD group). (**H**) Average swimming speed in testing phase caused by the indicated stimuli. (**I–K**) The crossing platform times, and the ratio of total time and distance spent in the targeted quadrant in the testing phase caused by the indicated stimuli. Data are presented as the mean ± SD (n = 6). *P <0.05, **P < 0.01, ***P <0.001, ****P <0.0001. Post-operative cognitive dysfunction (POCD) was initiated by a model of tibial fracture surgery. Vehicle: rats were only treated with a skin incision and suture on the left hind paw following anesthesia. EA and α-BGT are described above.
Abbreviation: Ns, not significant.

the platform in the POCD group from days 2–4 after AS (P <0.05; Figure 2F and G); however, the increased latency period to locate the submerged platform was noted in the α-BGT + EA + POCD-treated rats compared with the EA + POCD-treated rats from days 2–4 after AS (P <0.05; Figure 2F and G). In addition, the crossing platform times (P <0.0001), the total time (P <0.001), and the distance spent in the targeted quadrant (P <0.0001) in the POCD group were significantly decreased compared with rats those in the vehicle group (Figure 2I–K). It was also shown that EA pretreatment significantly increased the crossing platform times (P <0.01), the total time (P <0.01), and the distance spent in the targeted quadrant (P <0.001) compared with the POCD group (P <0.05; Figure 2I–K), while α-BGT partially reversed those changes (P <0.01; Figure 2I–K). There were no apparent differences in the latency period to locate the submerged platform, crossing platform times, total time, and distance spent in the targeted quadrant between aged rats in the POCD, EA + POCD, and α-BGT + EA +POCD groups (Figure 2I–K). In addition, there was no significant difference in the average swimming speed between rats in the above five groups (Figure 2H).

Electroacupuncture Pretreatment Ameliorates Neuronal Injury After AS in Aged Rats

The neuronal amount and apoptosis were assessed by Nissl staining and TUNEL assays. Our data showed that the neurons were in alignment, and the structure was complete in the dentate gyrus, but the neurons were disorganized after surgical exposure. EA pretreatment significantly restored the alignment and structure in the dentate gyrus, while α-BGT partially reversed the protective effects of EA. Also, Nissl bodies were remarkably decreased (P <0.0001), but TUNEL-positive neurons were increased (P <0.001) in the POCD group compared with Vehicle group (vs Vehicle group; Figure 3A–D). However, EA pretreatment restored the neuronal amount (P <0.01) but reduced TUNEL-positive neurons (P <0.001) in the EA + POCD group compared with POCD group (EA + POCD vs POCD groups, P <0.05; Figure 3A–D), while α-BGT partially reversed those (Nissl, P <0.05; TUNEL, P <0.0001; α-BGT + EA + POCD vs EA + POCD groups; Figure 3A–D). There was no difference in neuronal

amount and apoptosis between aged rats in the POCD, EA + POCD and α-BGT + EA +POCD groups.

Electroacupuncture Pretreatment Ameliorates Microglial Activation After AS in Aged Rats

Based on the activated morphology, as evidenced by expanded cell bodies and shortened branches, Sholl analysis was used to analyze the Iba1-positive cells in the dentate gyrus. Activated microglia, as indicated by the number of Iba1-positive cells (P <0.0001) and length of branches (P <0.0001), was significantly increased in rats exposed to tibial fracture surgery compared with vehicle exposure (Figure 4A–C). Note that EA pretreatment significantly decreased the number of activated microglia (P <0.0001) and restored the length of branches (P <0.0001) in the EA + POCD group microglia compared with the POCD group (P <0.0001; Figure 4A–C), whereas α-BGT partially reversed these changes in activated microglia (P <0.0001; Figure 4A–C). In addition, there was no difference in activated microglia between aged rats in the POCD, EA + POCD, and α-BGT + EA +POCD groups.

Electroacupuncture Pretreatment Ameliorates HMGB1 and Phosphor-NF-κB Expression in Microglia

HMGB1 and phosphor-NF-κB, vital regulators of neuroinflammatory factors, were detected in the microglia using immunofluorescence assays. It was shown that the percentages of HMGB1- (P <0.0001) and phosphor-NF-κB-positive (P <0.0001) microglia were significantly increased in aged rats after surgical treatment compared with rats exposed to vehicle (Figure 5A–D). Notably, we also showed that EA pretreatment significantly decreased HMGB1 combined with Iba1-positive cells (P <0.0001) and phosphor-NF-κB combined with Iba1-positive cells (P <0.0001) in the EA + POCD group compared with the POCD group (Figure 5A–D); however, α-BGT administration significantly reduced the percentages of HMGB1- (P <0.0001) and phosphor-NF-κB-positive (P <0.0001) microglia in the α-BGT + EA + POCD group compared with the EA + POCD group (Figure 5A–D). In addition, there was no difference in the percentages of HMGB1- and phosphor-NF-κB-positive microglia between aged rats in the POCD, EA + POCD, and α-BGT + EA +POCD groups.
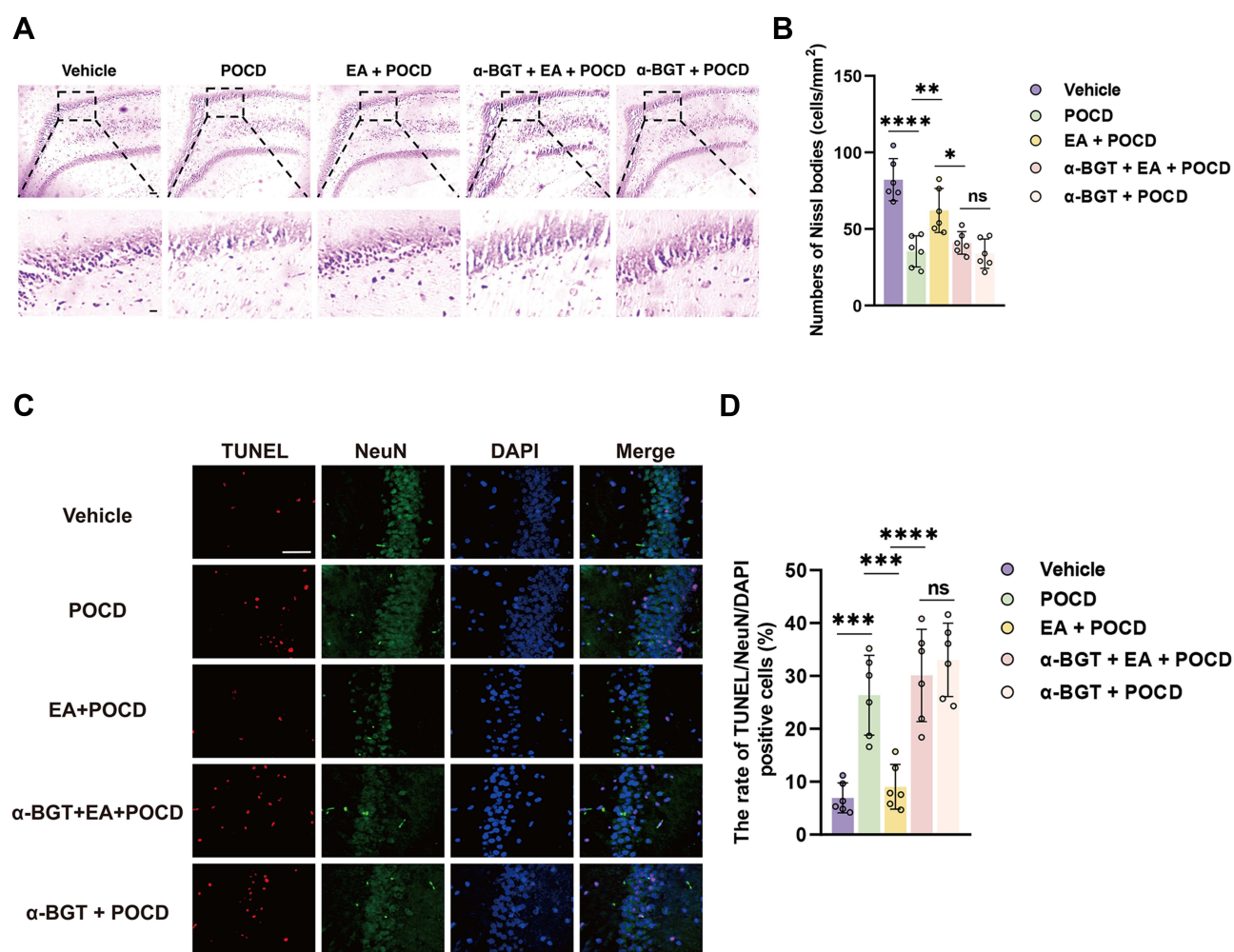
Figure 3 Electroacupuncture pretreatment ameliorates neuronal injury after AS in aged rats. (**A**) Representative photomicrographs of Nissl staining in the dentate gyrus caused by the indicated stimuli. Scale bar = 50 and 10 μm (**B**) The number of Nissl bodies was quantified with Nissl staining in the dentate gyrus. (**C**) Representative photomicrographs of TUNEL (specificity marker of apoptosis, red) plus NeuN (specificity marker of neuron, green) in the dentate gyrus caused by the indicated stimuli. Scale bar = 50 μm (**D**) The rate of TUNEL- and NeuN-positive cells in the dentate gyrus caused by the indicated stimuli. Data are presented as the mean ± SD (n = 6). *P <0.05, **P < 0.01, ***P <0.001, ****P <0.0001. Vehicle, POCD, EA, and α-BGT are described above.
Abbreviation: Ns, not significant.

Electroacupuncture Pretreatment Ameliorates the Expression of HMGB1 Downstream Factors After AS in Aged Rats

Furthermore, HMGB1 downstream inflammatory factors, including NF-κB, IL-6, and IL-1β in the hippocampus, were assessed using Western blot. The results of Western blot indicated that the expression of phospho-NF-κB (P <0.001), IL-6 (P <0.0001) and IL-1β (P <0.05), were statistically increased in rats exposed to tibial fracture surgery in the POCD group compared rats exposed to vehicle treatment (Figure 6A–D). Compared with rats in the POCD group, the rats in the EA + POCD group exhibited significantly reduced expression of phospho-NF-κB (P <0.001), IL-6 (P <0.0001)

and IL-1β (P <0.05) (Figure 6A–D). Again, each of these changes (phospho-NF-κB, P <0.001; IL-6, P <0.0001; IL-1β, P <0.05) was reversed by a-BGT (Figure 6A–D). In addition, there was no differences in expression of phospho-NF-κB, IL-6, and IL-1β in the hippocampus between aged rats in the POCD, EA + POCD and α-BGT + EA +POCD groups.

Discussion

The findings of the current study implicate α7-nAChR activation induced by EA pretreatment in the cognitive dysfunction process following tibial fracture surgery. Specifically, activation of α7-nAChR induced by EA significantly increased crossing platform times and the time with a novel object, restored the number of neurons, decreased TUNEL-positive neurons, alleviated activation
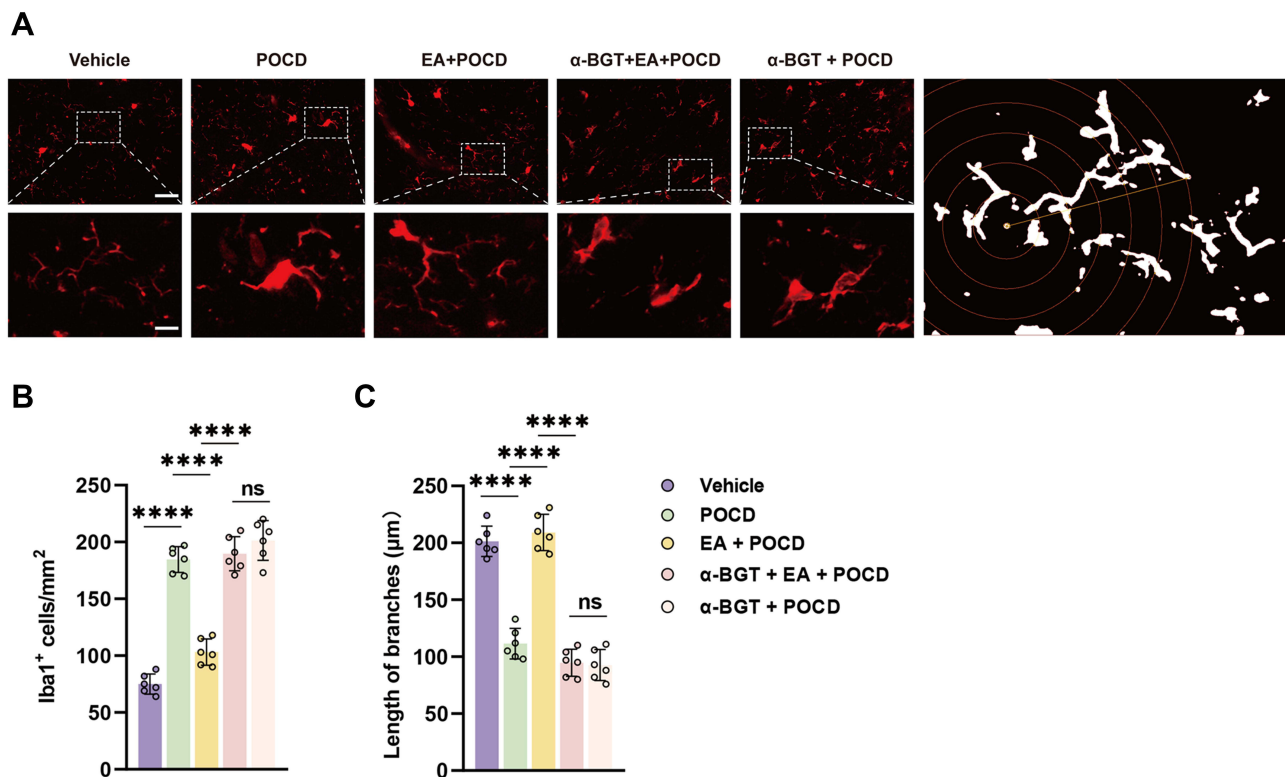
Figure 4 Electroacupuncture pretreatment ameliorates microglial activation after AS in aged rats. (**A**) Representative photomicrographs of Iba1 staining and Sholl analysis in the dentate gyrus caused by the indicated stimuli. Scale bar = 50 and 10 μm. (**B**) The number of Iba1-positive cells was quantified using an immunofluorescence assay. (**C**) The length of branches in Iba1-positive cells was quantified with an immunofluorescence assay. Data are presented as the mean ± SD (n = 6). ****P <0.0001. Vehicle, POCD, EA, and α-BGT are described above.
Abbreviation: Ns, not significant.

of microglia, downregulated expression of HMGB1 and NF-κB in the microglia, reduced levels of HMGB1-associated downstream factors, including NF-κB, IL-6, and IL-1β, while α-BGT partially reversed these changes. Overall, this study highlights a critical role for an α7-nAChR signal in regulating the neuroinflammatory response under POCD conditions.

A growing number of publications recommend that the clinical nomenclature for impairment in cognitive function that is temporally associated with anesthesia and/or surgery should be changed from POCD to PNDs.[2] This change better aligns these disorders with the phenotypically similar neurocognitive diagnoses listed in version 5 of the Diagnostic and Statistical Manual of Mental Disorders, such as Parkinson's and Alzheimer's diseases.[26] The preclinical examination of POCD indicates much in the way of mechanistic insight into cognitive changes after anesthesia and/or surgery, and several compelling hypotheses regarding neuroinflammation, inflammation resolution, and adverse anesthetic effects have emerged.[27] The relationship between perioperative

neurocognitive impairments and the surgery or anesthetic, however, is uncertain. Thus, the POCD nomenclature was used in this study. Here, tibial fracture surgery was selected to establish a model of POCD in aged rats. Growing evidence has reported that tibial fracture surgery can initiate the process of POCD and induce significant long-term effects on cognitive dysfunction.[28,29] Considering the influence of movement after surgery, behavioral tests, including the NOR and Morris maze tests 30 days after surgery, were chosen in this experiment. Interestingly, we found that tibial fracture surgery induced a significant cognitive decline, as indicated by an increased latency period to platform, decreased crossing platform times, and reduced time with a novel object, which was consistent with previous studies.[30,31] In addition, the pathologic changes indicated that the number of neurons was significantly decreased after tibial fracture surgery in the dentate gyrus. Our behavioral data revealed that in this POCD model, cognitive dysfunction was successfully initiated and the neuronal injury in the dentate gyrus may be relative to the POCD process.
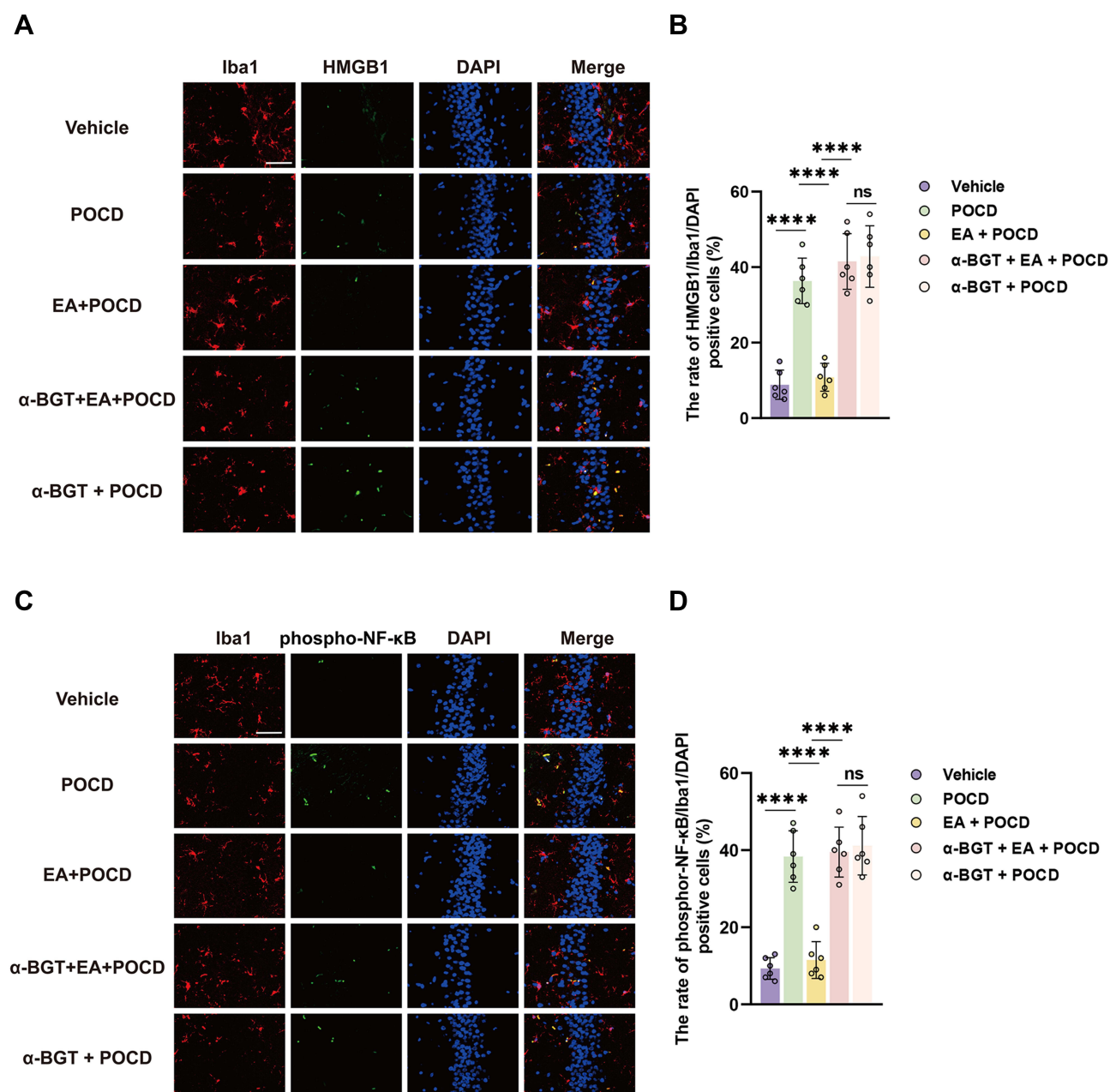
A

B

C

D

Figure 5 Electroacupuncture pretreatment ameliorates HMGB1 and phosphor-NF-κB expression in the microglia. (**A**) Representative photomicrographs of Iba1 (specificity marker of microglia) and HMGB1 plus DAPI staining in the dentate gyrus caused by the indicated stimuli. Scale bar = 50 μm. (**B**) The rate of HMGB1- and Iba1-positive cells in the dentate gyrus caused by the indicated stimuli. (**C**) Representative photomicrographs of Iba1 (specificity marker of microglia) and phosphor-NF-κB plus DAPI staining in the dentate gyrus caused by the indicated stimuli. Scale bar = 50 μm. (**D**) The rate of phosphor-NF-κB- and Iba1-positive cells in the dentate gyrus caused by the indicated stimuli. Data are presented as the mean ± SD (n = 6). ****P <0.0001. Vehicle, POCD, EA, and α-BGT are described above.
Abbreviation: Ns, not significant.

Microglia-associated neuroinflammation occurs in the progression of cognitive dysfunction after anesthesia and surgical treatment.[32] Previous studies have demonstrated that the inflammatory cascade induced by microglial activation results in significant micro-environment changes in the vital nucleus, thereby leading to neuronal degeneration.[33,34] Pro-inflammatory cytokines, including

IL-6 and IL-1β secreted from microglia, can result in neuronal injury and apoptosis in models of ischemia or infection.[35–37] Note that the activation of the HMGB1–NF-κB signal takes part in the upregulation of inflammatory cytokines.[38,39] In the current study, it was shown that activation of microglia, as indicated by increased branches and larger soma, was significantly increased after tibial
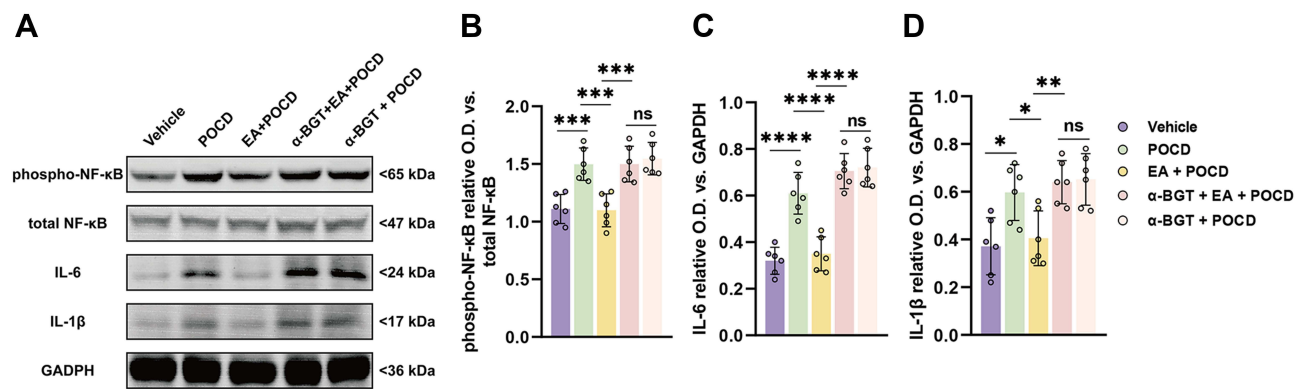
Figure 6 Electroacupuncture pretreatment ameliorates the expression of HMGB1 downstream factors after AS in aged rats. (**A**) Representative Western blot of phosphor-NF-κB (Ser536), total NF-κB, IL-6, and IL-1β in the dentate gyrus caused by the indicated stimuli. (**B**) The ratio between the optical density value of phosphor-NF-κB (Ser536) versus the total NF-κB in the dentate gyrus. (**C** and **D**) The ratio between the optical density value of IL-6 and IL-1β versus GAPDH in the dentate gyrus. Data are presented as the mean ± SD (n = 6). *P <0.05, **P < 0.01, ***P <0.001, ****P <0.0001. Vehicle, POCD, EA, and α-BGT are described above.
Abbreviation: Ns, not significant.

fracture surgery. We also found that the HMGB1–NF-κB signal in the microglia, as well as the expression of HMGB1-downstream factors, including IL-6 and IL-1β in the dentate gyrus, were elevated. These data revealed that activation of the HMGB1–NF-κB signal in the microglia might be involved in the development of cognitive dysfunction after anesthesia and surgical treatment.

Based on traditional Chinese medicine theory, Hegu, an original point of the large intestine meridian, is usually used to treat various diseases of the head and face.[40] Neiguan, one of the most critical points in our body, exerts potential therapeutical effects against mental and neurologic deficits.[41] In addition, Zusanli, a main acupoint of the "stomach meridian," has been reported to promote recovery from neurologic diseases.[42] In our previous study, we reported that EA pretreatment with Hegu, Neiguan, and Zusanli significantly alleviated postoperative cognitive decline in geriatric patients with silent lacunar infarctions[15] and in patients following spine surgery.[43] In the current study, we found that EA pretreatment with Hegu, Neiguan, and Zusanli in aged rats also significantly increased crossing platform times in the Morris maze test and elevated the time with a novel object in a model of tibial fracture surgery. In addition, EA pretreatment also restored the number of neurons, inhibited the activation of microglia, reduced the number of HMGB1- and NF-κB-positive microglia, and downregulated the expression of IL-6 and IL-1β in the dentate gyrus in this model of POCD. The above data indicate that the mechanism underlying EA pretreatment against POCD might be associated with inhibition of the HMGB1–NF-κB signal in the microglia.

Alpha7-nAChR, a cholinergic-dependent signal, has been reported to take part in a variety of neurologic diseases, including Parkinson's disease, Alzheimer's disease, and emotional changes.[44–46] When the α7-nAChR signal is blocked, cognitive functions, including exploring, memory, and learning, can be significantly worse in surgical mice after general anesthesia.[47] Interestingly, we found that α-BGT, a selective antagonist of α7-nAChR, partially reversed the neuroprotective effects of EA pretreatment against cognitive dysfunction after tibial fracture surgery. In addition, α-BGT significantly reduced the number of neurons, increased the number of activated microglia, upregulated expression of the HMGB1–NF-κB signal associated factors, including HMGB1, phosphor-NF-κB, IL-6, and IL-1β. The expression of α7-nAChR in the microglia was significantly reduced after chronic stress.[48] In addition, the α7-nAChR plays an essential role in the cholinergic anti-inflammatory pathway that regulates macrophage/microglia function in inflammation.[49] Farré-Alins et al[50] reported that α7-nAChR increases autophagic flux via regulation of the NLRP3 inflammasome and inhibition of reactive oxygen species (ROS), which subsequently regulates the HMGB1–NF-κB signal.[51,52] Previous studies[48,50] and our findings revealed that α7-nAChR in the microglia may be the upstream signaling pathway of anesthesia plus surgical stress-induced cognitive impairment. Also, α7-nAChR might mediate decreased microglial activation in the dentate gyrus, thus causing cerebral inflammation and cognitive dysfunction after perioperative stress in aged rats.

Several limitations of the current study should be mentioned. First, we performed only one model of POCD in this current study. Other POCD models in aged rats, such as

splenectomy and partial hepatectomy, should be further investigated. In addition, not only Hegu, Neiguan, and Zusanli, but other acupoints should be studied. Therefore, more efforts are required to further explore the potential mechanism underlying EA pretreatment against POCD other than inflammation.

This study determined the role and exact mechanism underlying EA pretreatment under POCD conditions. Our data indicated that EA pretreatment improved cognitive dysfunction in aged rats after anesthesia and surgical treatment, and the mechanism may be relative to inhibition of HMGB-1–NF-κB induced by activation of the α7-nAChR signal in the hippocampus.

Acknowledgment

Disclosure

The authors have no conflicts of interest to declare.

References

1. Evered LA, Silbert BS. Postoperative cognitive dysfunction and non-cardiac surgery. *Anesth Analg*. 2018;127:496–505. doi:10.1213/ane.0000000000003514
2. Evered L, Silbert B, Knopman DS, et al. Recommendations for the nomenclature of cognitive change associated with anaesthesia and surgery—2018. *Br J Anaesth*. 2018;121(5):1005–1012. doi:10.1016/j.bja.2017.11.087
3. Urits I, Orhurhu V, Jones M, et al. Current perspectives on postoperative cognitive dysfunction in the ageing population. *Turk J Anaesthesiol Reanim*. 2019;47(6):439–447. doi:10.5152/tjar.2019.75299
4. Rundshagen I. Postoperative cognitive dysfunction. *Dtsch Arztebl Int*. 2014;111:119–125. doi:10.3238/arztebl.2014.0119
5. Evered L, Scott DA, Silbert B. Cognitive decline associated with anesthesia and surgery in the elderly: does this contribute to dementia prevalence? *Curr Opin Psychiatry*. 2017;30(3):220–226. doi:10.1097/yco.0000000000000321
6. Skvarc DR, Berk M, Byrne LK, et al. Post-operative cognitive dysfunction: an exploration of the inflammatory hypothesis and novel therapies. *Neurosci Biobehav Rev*. 2018;84:116–133. doi:10.1016/j.neubiorev.2017.11.011
7. Alam A, Hana Z, Jin Z, Suen KC, Ma D. Surgery, neuroinflammation and cognitive impairment. *EBioMedicine*. 2018;37:547–556. doi:10.1016/j.ebiom.2018.10.021
8. Wang Z, Meng S, Cao L, et al. Critical role of NLRP3-caspase-1 pathway in age-dependent isoflurane-induced microglial inflammatory response and cognitive impairment. *J Neuroinflammation*. 2018;15(1):109. doi:10.1186/s12974-018-1137-1
9. Yang LH, Xu YC, Zhang W. Neuroprotective effect of CTRP3 over-expression against sevoflurane anesthesia-induced cognitive dysfunction in aged rats through activating AMPK/SIRT1 and PI3K/AKT signaling pathways. *Eur Rev Med Pharmacol Sci*. 2020;24:5091–5100. doi:10.26355/eurrev_202005_21202

10. Kotekar N, Shenkar A, Nagaraj R. Postoperative cognitive dysfunction - current preventive strategies. *Clin Interv Aging*. 2018;13:2267–2273. doi:10.2147/cia.S133896
11. Kamuf J, Garcia Bardon A, Ziebart A, et al. Experimental lung injury induces cerebral cytokine mRNA production in pigs. *PeerJ*. 2020;8:e10471. doi:10.7717/peerj.10471
12. Tang Y, Wang T, Yang L, et al. Acupuncture for post-operative cognitive dysfunction: a systematic review and meta-analysis of randomized controlled trials. *Acupunct Med*. 2020:964528420961393. doi:10.1177/0964528420961393
13. Liu P-R, Zhou Y, Zhang Y, Diao S. Electroacupuncture alleviates surgery-induced cognitive dysfunction by increasing α7-nAChR expression and inhibiting inflammatory pathway in aged rats. *Neurosci Lett*. 2017;659:1–6. doi:10.1016/j.neulet.2017.08.043
14. Han Y-G, Qin X, Zhang T, et al. Electroacupuncture prevents cognitive impairment induced by lipopolysaccharide via inhibition of oxidative stress and neuroinflammation. *Neurosci Lett*. 2018;683:190–195. doi:10.1016/j.neulet.2018.06.003
15. Gao F, Zhang Q, Li Y, et al. Transcutaneous electrical acupoint stimulation for prevention of postoperative delirium in geriatric patients with silent lacunar infarction: a preliminary study. *Clin Interv Aging*. 2018;13:2127–2134. doi:10.2147/cia.S183698
16. Gaidhani N, Uteshev VV. Treatment duration affects cytoprotective efficacy of positive allosteric modulation of α7 nAChRs after focal ischemia in rats. *Pharmacol Res*. 2018;136:121–132. doi:10.1016/j.phrs.2018.09.001
17. Sun F, Jin K, Uteshev VV, Mongin A. A type-II positive allosteric modulator of α7 nAChRs reduces brain injury and improves neurological function after focal cerebral ischemia in rats. *PLoS One*. 2013;8(8):e73581. doi:10.1371/journal.pone.0073581
18. Mei Z, Tian X, Chen J, et al. α7-nAChR agonist GTS-21 reduces radiation-induced lung injury. *Oncol Rep*. 2018;40:2287–2297. doi:10.3892/or.2018.6616
19. Ibrahim SM, Al-Shorbagy MY, Abdallah DM, El-Abhar HS. Activation of α7 nicotinic acetylcholine receptor ameliorates zymosan-induced acute kidney injury in BALB/c mice. *Sci Rep*. 2018;8(1):16814. doi:10.1038/s41598-018-35254-1
20. Xia YY, Xue M, Wang Y, Huang ZH, Huang C. Electroacupuncture alleviates spared nerve injury-induced neuropathic pain and modulates HMGB1/NF-κB signaling pathway in the spinal cord. *J Pain Res*. 2019;12:2851–2863. doi:10.2147/jpr.S220201
21. Feng -P-P, Deng P, Liu L-H, et al. Electroacupuncture alleviates postoperative cognitive dysfunction in aged rats by inhibiting hippocampal neuroinflammation activated via microglia/TLRs pathway. *Evid Based Complement Alternat Med*. 2017;2017:6421260. doi:10.1155/2017/6421260
22. Yan J, Luo A, Gao J, et al. The role of SIRT1 in neuroinflammation and cognitive dysfunction in aged rats after anesthesia and surgery. *Am J Transl Res*. 2019;11:1555–1568.
23. Zhang L, Wang H, Huang Z, et al. Inhibiting effect of electroacupuncture at zusanli on early inflammatory factor levels formed by postoperative abdominal adhesions. *Evid Based Complement Alternat Med*. 2014;2014:950326. doi:10.1155/2014/950326
24. Jiang XL, Gu XY, Zhou XX, et al. Intestinal dysbacteriosis mediates the reference memory deficit induced by anaesthesia/surgery in aged mice. *Brain Behav Immun*. 2019;80:605–615. doi:10.1016/j.bbi.2019.05.006
25. Qiao LN, Liu JL, Tan LH, et al. Effect of electroacupuncture on thermal pain threshold and expression of calcitonin-gene related peptide, substance P and γ-aminobutyric acid in the cervical dorsal root ganglion of rats with incisional neck pain. *Acupunct Med*. 2017;35:276–283. doi:10.1136/acupmed-2016-011177
26. Eckenhoff RG, Maze M, Xie Z, et al. Perioperative neurocognitive disorder: state of the preclinical science. *Anesthesiology*. 2020;132(1):55–68. doi:10.1097/aln.0000000000002956

27. Subramaniyan S, Terrando N. Neuroinflammation and perioperative neurocognitive disorders. *Anesth Analg*. 2019;128(4):781–788. doi:10.1213/ane.0000000000004053

28. Netto MB, de Oliveira Junior AN, Goldim M, et al. Oxidative stress and mitochondrial dysfunction contributes to postoperative cognitive dysfunction in elderly rats. *Brain Behav Immun*. 2018;73:661–669. doi:10.1016/j.bbi.2018.07.016

29. Li P-J, Guo Y-Q, Ding P-Y, et al. Neuroprotective effects of a smoothened receptor agonist against postoperative cognitive dysfunction by promoting autophagy in the dentate gyrus of aged rats. *Neurol Res*. 2019;41(10):867–874. doi:10.1080/01616412.2019.1628411

30. Meng B, Li X, Lu B, et al. The investigation of hippocampus-dependent cognitive decline induced by anesthesia/surgery in mice through integrated behavioral Z-scoring. *Front Behav Neurosci*. 2020;13:282. doi:10.3389/fnbeh.2019.00282

31. Zhang X, Jiang X, Huang L, et al. Central cholinergic system mediates working memory deficit induced by anesthesia/surgery in adult mice. *Brain Behav*. 2018;8(5):e00957. doi:10.1002/brb3.957

32. Chen L, Dong R, Lu Y, et al. MicroRNA-146a protects against cognitive decline induced by surgical trauma by suppressing hippocampal neuroinflammation in mice. *Brain Behav Immun*. 2019;78:188–201. doi:10.1016/j.bbi.2019.01.020

33. Norris GT, Smirnov I, Filiano AJ, et al. Neuronal integrity and complement control synaptic material clearance by microglia after CNS injury. *J Exp Med*. 2018;215(7):1789–1801. doi:10.1084/jem.20172244

34. Suzumura A. Neuron-microglia interaction in neuroinflammation. *Curr Protein Pept Sci*. 2013;14:16–20. doi:10.2174/1389203711314010004

35. Lambertsen KL, Finsen B, Clausen BH. Post-stroke inflammation-target or tool for therapy? *Acta Neuropathol*. 2019;137:693–714. doi:10.1007/s00401-018-1930-z

36. Diaz-Cañestro C, Reiner MF, Bonetti NR, et al. AP-1 (activated protein-1) transcription factor JunD regulates ischemia/reperfusion brain damage via IL-1β (Interleukin-1β). *Stroke*. 2019;50(2):469–477. doi:10.1161/strokeaha.118.023739

37. Patterson SL. Immune dysregulation and cognitive vulnerability in the aging brain: interactions of microglia, IL-1β, BDNF and synaptic plasticity. *Neuropharmacology*. 2015;96:11–18. doi:10.1016/j.neuropharm.2014.12.020

38. Liu C, Zha X, Liu H, Wei F, Zhang F. Ampelopsin alleviates sevoflurane-induced cognitive dysfunction by mediating NF-κB pathway in aged rats. *Genes Genomics*. 2020;42(4):361–369. doi:10.1007/s13258-019-00897-5

39. Wei P, Zheng Q, Liu H, et al. Nicotine-induced neuroprotection against cognitive dysfunction after partial hepatectomy involves activation of BDNF/TrkB signaling pathway and inhibition of NF-κB signaling pathway in aged rats. *Nicotine Tob Res*. 2018;20(4):515–522. doi:10.1093/ntr/ntx157

40. Chavez LM, Huang -S-S, MacDonald I, et al. Mechanisms of acupuncture therapy in ischemic stroke rehabilitation: a literature review of basic studies. *Int J Mol Sci*. 2017;18(11):2270. doi:10.3390/ijms18112270

41. Yin J, Yang M, Yu S, et al. Effect of acupuncture at neiguan point combined with amiodarone therapy on early recurrence after pulmonary vein electrical isolation in patients with persistent atrial fibrillation. *J Cardiovasc Electrophysiol*. 2019;30(6):910–917. doi:10.1111/jce.13924

42. Sun Z-G, Pi Y-L, Zhang J, et al. Effect of acupuncture at ST36 on motor cortical excitation and inhibition. *Brain Behav*. 2019;9(9):e01370. doi:10.1002/brb3.1370

43. Zhang Q, Li Y-N, Guo -Y-Y, et al. Effects of preconditioning of electro-acupuncture on postoperative cognitive dysfunction in elderly: a prospective, randomized, controlled trial. *Medicine*. 2017;96(26):e7375. doi:10.1097/md.0000000000007375

44. Stuckenholz V, Bacher M, Balzer-Geldsetzer M, et al. The α7 nAChR agonist PNU-282987 reduces inflammation and MPTP-induced nigral dopaminergic cell loss in mice. *J Parkinsons Dis*. 2013;3(2):161–172. doi:10.3233/jpd-120157

45. Stoiljkovic M, Kelley C, Hajós GP, et al. Hippocampal network dynamics in response to α7 nACh receptors activation in amyloid-β overproducing transgenic mice. *Neurobiol Aging*. 2016;45:161–168. doi:10.1016/j.neurobiolaging.2016.05.021

46. Morales M, Hein K, Vogel Z. Hippocampal interneurons co-express transcripts encoding the α7 nicotinic receptor subunit and the cannabinoid receptor 1. *Neuroscience*. 2008;152(1):70–81. doi:10.1016/j.neuroscience.2007.12.019

47. Yin J, Zhao X, Wang L, et al. Sevoflurane-induced inflammation development: involvement of cholinergic anti-inflammatory pathway. *Behav Pharmacol*. 2019;30(8):730–737. doi:10.1097/fbp.0000000000000507

48. Xue R, Wan Y, Sun X, et al. Nicotinic mitigation of neuroinflammation and oxidative stress after chronic sleep deprivation. *Front Immunol*. 2019;10:2546. doi:10.3389/fimmu.2019.02546

49. Zhang Q, Lu Y, Bian H, Guo L, Zhu H. Activation of the α7 nicotinic receptor promotes lipopolysaccharide-induced conversion of M1 microglia to M2. *Am J Transl Res*. 2017;9:971–985.

50. Farré-Alins V, Narros-Fernández P, Palomino-Antolín A, et al. Melatonin reduces NLRP3 inflammasome activation by increasing α7 nAChR-mediated autophagic flux. *Antioxidants*. 2020;9(12):1299. doi:10.3390/antiox9121299

51. Jia C, Zhang J, Chen H, et al. Endothelial cell pyroptosis plays an important role in Kawasaki disease via HMGB1/RAGE/cathespin B signaling pathway and NLRP3 inflammasome activation. *Cell Death Dis*. 2019;10(10):778. doi:10.1038/s41419-019-2021-3

52. Ye Y, Jin T, Zhang X, et al. Meisoindigo protects against focal cerebral ischemia-reperfusion injury by inhibiting NLRP3 inflammasome activation and regulating microglia/macrophage polarization via TLR4/NF-κB signaling pathway. *Front Cell Neurosci*. 2019;13:553. doi:10.3389/fncel.2019.00553